Recognition of acetylated histone by Yaf9 regulates metabolic cycling of transcription initiation and chromatin regulatory factors

Jibo Zhang,[1] Aakanksha Gundu,[1] and Brian D. Strahl[1,2]

[1]Department of Biochemistry and Biophysics, School of Medicine, University of North Carolina at Chapel Hill, Chapel Hill, North Carolina 27599, USA; [2]Lineberger Comprehensive Cancer Center, School of Medicine, University of North Carolina at Chapel Hill, Chapel Hill, North Carolina 27599, USA

How transcription programs rapidly adjust to changing metabolic and cellular cues remains poorly defined. Here, we reveal a function for the Yaf9 component of the SWR1-C and NuA4 chromatin regulatory complexes in maintaining timely transcription of metabolic genes across the yeast metabolic cycle (YMC). By reading histone acetylation during the oxidative and respiratory phase of the YMC, Yaf9 recruits SWR1-C and NuA4 complexes to deposit H2A.Z and acetylate H4, respectively. Increased H2A.Z and H4 acetylation during the oxidative phase promotes transcriptional initiation and chromatin machinery occupancy and is associated with reduced RNA polymerase II levels at genes—a pattern reversed during transition from oxidative to reductive metabolism. Prevention of Yaf9-H3 acetyl reading disrupted this pattern of transcriptional and chromatin regulator recruitment and impaired the timely transcription of metabolic genes. Together, these findings reveal that Yaf9 contributes to a dynamic chromatin and transcription initiation factor signature that is necessary for the proper regulation of metabolic gene transcription during the YMC. They also suggest that unique regulatory mechanisms of transcription exist at distinct metabolic states.

[*Keywords*: yeast metabolic cycle; Yaf9; histone; histone acetylation; YEATS domain; NuA4; SWR1-C; chromatin regulatory complexes; H2A.Z; transcription]

Supplemental material is available for this article.

Received August 5, 2021; revised version accepted November 2, 2021.

Histone post-translational modifications (PTMs), chromatin remodeling enzymes, and histone variants have crucial functions in DNA-templated processes, such as gene transcription, DNA repair, and DNA replication (Strahl and Allis 2000; Talbert and Henikoff 2021). In large part, distinct epigenetic landscapes are established and maintained by enzymes and/or protein complexes that install, remove, and/or read histone PTMs and histone variants (Gardner et al. 2011; Henikoff and Smith 2015). How these landscapes become generated and contribute to the DNA-templated processes they regulate are still incompletely understood.

Although the regulatory mechanisms that contribute to chromatin regulation are yet to be fully explained, recent advances have greatly expanded our understanding of the range of histone modifications and the types of protein domains that read them (Rothbart and Strahl 2014; Li et al. 2017). For example, the YEATS domain is a newly recognized reader module that associates with histone lysine acetylation and other forms of acylation (e.g., lysine crotonylation) (Andrews et al. 2016a; Li et al. 2017; Zhao et al. 2017). Some YEATS domain-containing proteins prefer to bind to histone crotonylation (e.g., Taf14 in yeast and AF9, ENL and YEATS2 in humans), whereas other YEATS proteins such as that found in GAS41 do not greatly distinguish lysine acetylation from crotonylation (Andrews et al. 2016b; Li et al. 2016; Zhang et al. 2016; Zhao et al. 2016).

Long-standing evidence points to a positive function for histone acetylation in promoting gene activity (Allfrey et al. 1964; Verdin and Ott 2015; Barnes et al. 2019); however, the function of histone crotonylation is less well established. Studies with mammalian cells show how p300-mediated crotonylation at H3K18 functions to recruit the AF9 YEATS domain in the superelongation complex to potentiate gene transcription (Sabari et al. 2015; Li et al. 2016). Conversely, studies with budding yeast show that Taf14 binding of histone crotonylation at H3K9 is

Corresponding author: brian_strahl@med.unc.edu
Article published online ahead of print. Article and publication date are online at http://www.genesdev.org/cgi/doi/10.1101/gad.348904.121.

associated with the timely repression of progrowth genes during a low-energy and reductive metabolic period in which β-oxidation and longer acyl-CoAs such as crotonyl-CoA are produced (Gowans et al. 2019). These examples highlight the diverse ways histone crotonylation can function, which is likely context- and YEATS domain-dependent.

Yaf9, a founding member of the YEATS domain family (i.e., Yaf9, ENL, AF9, Taf14, and Sas5), is associated within two major catalytically conserved complexes that act on chromatin; namely, the NuA4 acetyltransferase that targets histones H4, H2A, and H2A.Z, and the SWR1-C ATP-dependent chromatin remodeling complex that deposits H2A.Z at gene promoters (Fig. 1A; Kobor et al. 2004; Mizuguchi et al. 2004; Zhang et al. 2004; Altaf et al. 2010; Klein et al. 2018b). Yaf9 is important to the function of both complexes and contributes to the transcriptional regulation and in DNA repair activities of NuA4 and SWR1-C (Schulze et al. 2010; Gerhold et al. 2015). The function of the YEATS domain in Yaf9 is less understood, but studies show that it can interact with H3K9ac and H3K27ac and contribute to the H2A.Z deposition function of SWR1-C (Wang et al. 2009; Klein et al. 2018b). Consistent with what has been observed in yeast, the human homolog of Yaf9, Gas41, has been found to promote H2A.Z deposition and associate with H3K14ac and H3K27ac on the promoters of active genes to regulate stem cell identify and lung cancer cell growth (Hsu et al. 2018a, b). Despite these advances, how the YEATS domain of Yaf9 and Gas41 regulate the activities of the complexes they are found in is still incompletely understood.

The yeast metabolic cycle (YMC) is a powerful system to examine how metabolic changes signal to chromatin and lead to transcriptional changes (Klevecz et al. 2004; Tu et al. 2005; Tu and McKnight 2007; Mellor 2016). Under continuous and glucose-limiting growth conditions, yeast becomes metabolically synchronized and oscillates through cycles of oxidative metabolism (i.e., respiration) known as the high oxygen consumption phase (HOC) followed by periods of reductive metabolism known as the low oxygen consumption phase (LOC) (Tu and McKnight 2007; Mellor 2016). This system closely resembles the nutrient-limiting conditions found in the wild and has direct ties with circadian rhythm, which itself is underpinned by metabolic processes (Tu and McKnight 2006). A key feature of cells that oscillate through the HOC phase is high energy and acetyl-CoA production that fuel the high energy needs of, e.g., ribosome and nucleic acid biosynthesis, progrowth activities that are initiated with available glucose (Tu et al. 2007). Conversely, the LOC phase is associated with cessation of oxygen consumption and is a period marked by cell division, stress response, β-oxidation, and autophagy (Tu et al. 2007). The HOC and LOC phases can be further subdivided into additional subphases based on gene expression and GO profiles (oxidative phase [OX], reductive building [RB] phase, and reductive charging [RC] phase) (Tu et al. 2005; Mellor 2016). Significantly, the LOC phase of the YMC is the period in which long-chain fatty acids are metabolized into additional acyl-CoA that includes crotonyl-CoA that provides the cofactor for histone crotonylation (Hiltunen et al. 2003; Mellor 2016; Gowans et al. 2019). We showed that, although histone acetylation is associated with the HOC phase of the YMC, histone crotonylation occurs in the LOC phase and, by the action of Taf14, is responsible for the repression of progrowth genes as cells transition from the HOC to the LOC stages (Gowans et al. 2019). Although we also found that the YEATS domain of Taf14 mediates the timely repression of progrowth genes, we did not know whether other YEATS domain-containing proteins in yeast also contribute to metabolic gene regulation.

In this report, we describe an important function of Yaf9 in metabolic gene regulation and control of the YMC. We show that Yaf9 is essential for the formation of YMC, and loss of its H3-acetyl interaction results in defects in the timing of the YMC and proper expression of metabolic genes. Mechanistically, we found that the YEATS domain of Yaf9 contributes to the recruitment of its associated complexes, SWR1-C and NuA4, to enable the deposition of H2A.Z and H4 acetylation during the oxidative phase of the YMC. Recruitment of SWR1-C and NuA4 to genes occurred globally with additional transcriptional initiation and chromatin factors, and this signature was associated with relatively low RNA polymerase II (Pol II) levels. Surprisingly, the loss of histone acetylation normally observed during transition into the LOC phase was further associated with globally low levels of SWR1-C and NuA4 and other initiation machinery but higher levels Pol II, a pattern that was largely the reverse of the HOC pattern. We posit that, during metabolic cycling, different energy requirements and nutrient availabilities fuel distinct patterns of chromatin modifications and transcriptional initiation machinery recruitment to genes that control how the distinct transcription programs found at these different metabolic states (e.g., HOC vs. LOC) are regulated.

Results

Yaf9 and its YEATS domain are crucial for proper progression of the yeast metabolic cycle

Yaf9 is a component of the NuA4 and SWR1-C chromatin regulatory complexes that install H2A and H4 N-terminal tail acetylation and incorporate H2A.Z, respectively (Fig. 1A,B). Yaf9 contains an evolutionarily conserved YEATS domain, and, although studies illustrate the ability of the Yaf9 YEATS domain to bind to histone acetylation, less is known about binding of the YEATS domain to other forms of histone acylation. To further interrogate the histone binding preferences of Yaf9, we purified a GST fusion of full-length Yaf9 (GST-Yaf9) and performed a series of solution-based peptide pull-down assays with histone H3 peptides that contained distinct forms of H3K9 or H3K27 acylation. In agreement with previous findings, the YEATS domain of Yaf9 showed robust interaction with H3 peptides that were acetylated at either H3K9 (H3K9ac) or H3K27 (H3K27ac) (Fig. 1C; Klein et al. 2018a). Intriguingly, the Yaf9 YEATS domain also

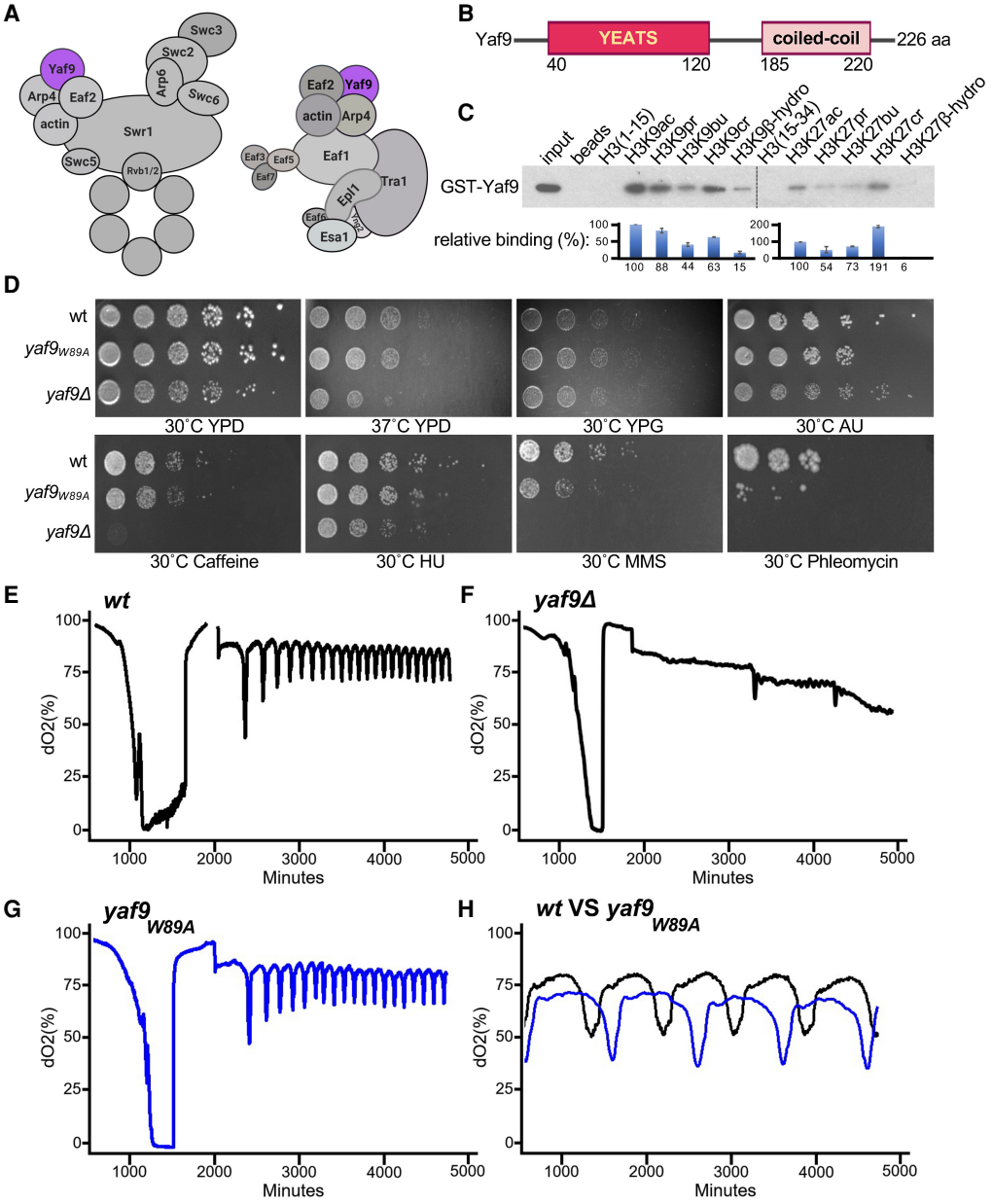

Figure 1. Yaf9 and its YEATS domain are crucial for proper YMC progression. (*A*) Schematic representations of the Yaf9-containing SWR1-C and NuA4 complexes. (*B*) Schematic representation of Yaf9. (*C*) Pull-down assays using histone H3 peptides and purified GST-tagged Yaf9 with the indicated acylated or unacylated peptides (residues 1–15 and 15–34 of the H3 tail). The bar graph *below* represents the quantitation of the pull-downs in which Yaf9 binding to H3K9ac or H3K27ac was normalized to 100% for comparison with other acylation peptide interactions. Standard deviation of independent triplicates is shown. (*D*) Growth of serially diluted wild-type, $yaf9_{W89A}$, and *yaf9Δ* strains on media containing various genotoxic agents or glycerol. (*E*) YMC profile for wild type under 0.15% glucose. (*F*) YMC profile for $yaf9_{W89A}$ under 0.15% glucose. (*G*) YMC profile for *yaf9Δ* under 0.15% glucose. (*H*) Overlapped YMC profile of wild type (black line) and $yaf9_{W89A}$ (blue line). The $yaf9_{W89A}$ strain shows an average elongated YMC of 30 min per cycle.

interacted with crotonylated H3K9 and H3K27 (H3K9cr and H3K27cr), albeit with efficiencies similar to or less than binding to H3K9ac and H3K27ac. Other forms of histone acylation at H3K9 and H3K27 (i.e., propionylation [pr], butyrylation [bu], and β-hydroxyisobutyrylation [β-hydro]) were tolerated less compared with acetylation or crotonylation. These data reveal that Yaf9 can recognize several major forms of histone acylation that normally partition to distinct phases of the yeast metabolic cycle (YMC) (Gowans et al. 2019).

Studies of the function of a related YEATS-containing protein, Taf14, revealed a critical function for the YEATS domain in metabolic gene regulation and timely progression of the YMC. To assess a possible contribution of Yaf9 and its YEATS domain to metabolic gene regulation and the YMC, we generated yeast strains in the

prototrophic CEN.PK background that were either deleted of *YAF9* (*yaf9Δ*) or had a mutation in its YEATS domain that abolished all histone acyl-lysine binding (*yaf9$_{W89A}$*) (Klein et al. 2018a). First, we confirmed that the strains grew on a glycerol-containing medium (YPG plates), which verified that the strains had intact mitochondria for proper metabolic cycling (Fig. 1D). We also examined the *yaf9Δ* and *yaf9$_{W89A}$* mutant strains for additional growth phenotypes. As shown in Figure 1D, the *yaf9Δ* and *yaf9$_{W89A}$* strains showed similar growth rates on yeast extract–peptone–dextrose (YPD) medium at 30˚C; only *yaf9Δ* cells showed slight temperature sensitivity at 37˚C on YPD plates. We next examined the *yaf9Δ* and *yaf9$_{W89A}$* mutant strains for growth on media containing a variety of genotoxic agents that report on defects in DNA replication (hydroxyurea [HU]), DNA damage repair (phleomycin and methanesulfonate [MMS]), nutrient signaling (caffeine), and transcription (6-azauracil). These experiments revealed that the complete absence of Yaf9 caused mild to severe growth defects on all the genotoxic agents tested. However, unlike the complete absence of Yaf9, mutations in its YEATS domain that blocked histone interaction caused growth phenotypes only on media containing DNA-damaging agents (Fig. 1D). These studies reinforced the important function of Yaf9 in many DNA-templated processes. The results also revealed a significant function for the Yaf9 YEATS domain in DNA repair.

The phenotypic assays described above, and previous studies of Yaf9, were performed in nutrient-rich conditions that can hide important functions for proteins and domains, such as the YEATS domain, that contribute to metabolic gene regulation. To assess a function of Yaf9 and its YEATS domain in metabolic-associated events, we used a continuous culture system wherein yeast cells were synchronized at the metabolic level and cycled through periods of high oxygen consumption (HOC) and low oxygen consumption (LOC) when grown under limiting glucose concentration (Klevecz et al. 2004; Tu et al. 2005). As shown in Figure 1E, the wild-type CEN.PK cells exhibited a typical metabolic cycle with an average cycle time of ~4 h. In stark contrast, the *yaf9Δ* strain failed to cycle under the same conditions, which indicated an essential requirement for Yaf9 in proper progression of the YMC (Fig. 1F). Intriguingly, the histone-blocking mutation of Yaf9 (*yaf9$_{W89A}$*) resulted in an altered metabolic cycle that was ~30 min longer than the matched wild-type strain (Fig. 1F,H). These findings indicated an important function for Yaf9 and histone acylation binding in metabolic cycling in a nutrient-limited environment.

H2a.Z and H4 acetylation oscillate across the YMC, and their levels are regulated by Yaf9-H3 acyl reading

Because of the altered YMC timing observed for the *yaf9$_{W89A}$* mutant strain, we next asked whether the prevention of Yaf9 association with histone acylation might affect the downstream activities of NuA4 and Swr1 that incorporate H4 N-terminal tail acetylation (H4ac) and/or H2A.Z, respectively. We collected wild-type or *yaf9$_{W89A}$* mutant cells at multiple time points across the YMC (Fig. 2A) and interrogated them for global levels of H4ac, H2A.Z, and other histone PTMs known to be regulated across the YMC (e.g., H3K9cr and H4K16ac). Samples were matched carefully so that all comparisons between the wild-type and *yaf9$_{W89A}$* strains were performed at identical locations during their HOC and LOC phases (depicted as time points 1–9). In addition, we also confirmed the specificity of our H2A.Z and H4ac antibodies (Supplemental Fig. S1A). As shown in Figure 2B, the general levels of core histones (H2A, H3, and H4) and a control cytosolic protein, glucose-6-phosphate dehydrogenase (G6PDH), did not change across the YMC in either the wild-type or *yaf9$_{W89A}$* mutant cells. As expected, the occurrence of H3K9ac, H4K16, and H4ac was highest in the HOC phase (time points 2–5) and decreased during the LOC phase of the YMC when H3K9cr levels peak (time points 6–9) in wild-type cells. Surprisingly, we also observed that the global incorporation of H2A.Z also cycled across the YMC, with the highest levels occurring during the HOC phase. We note that H2A.Z metabolic cycling and genome-wide global shifts in a histone variant such as H2A.Z have not been reported; however, such increases of H2A.Z at the HOC phase would be consistent with the observation of high levels of histone acetylation during the HOC phase that could recruit and/or stimulate Swr1 to increase H2A.Z deposition (Kobor et al. 2004; Zhang et al. 2004). Finally, analysis of the histone and histone PTM patterns from *yaf9$_{W89A}$* cells revealed that they were largely the same as observed in wild-type cells, albeit the levels of H4ac and H2A.Z appeared to be reduced.

Because of the apparent overall reduction of H4ac and H2A.Z levels in *yaf9$_{W89A}$* cells, we next performed a side-by-side immunoblot comparison of the wild-type and *yaf9$_{W89A}$* strains at three time points that represented either the transition point between the LOC and HOC phase (time point 1) or the peaks of the HOC or LOC phases (time points 2 and 3, respectively) (Fig. 2C). As shown in Figure 2D, and further quantified in Figure 2, E and F, the global levels of H2A.Z and H4ac were significantly reduced in the *yaf9$_{W89A}$* strain, whereas other histones and Pol II levels were unaffected. These findings demonstrated that Yaf9-H3 acyl reading was important for proper deposition of H2A.Z and H4ac across the YMC, which implied an important function for the Yaf9 YEATS domain in NuA4 and Swr1 activity.

The YEATS domain of Yaf9 is required for precise metabolic gene transcription

Because the Yaf9 YEATS domain was required for proper YMC timing and for the maintenance of H2A.Z and H4 acetylation levels in chromatin, we next asked how the absence of Yaf9-H3 acyl reading affected metabolic and global gene transcription. We performed RNA-seq for our wild-type and *yaf9$_{W89A}$* cells across three consecutive YMCs (Fig. 3A,B). Five time points within each cycle were collected and selected to represent the transition into the HOC phase (time points 1 and 2), the transition into the LOC phase (time points 3 and 4), and transition into the quiescent-like LOC phase (time point 5). Principal

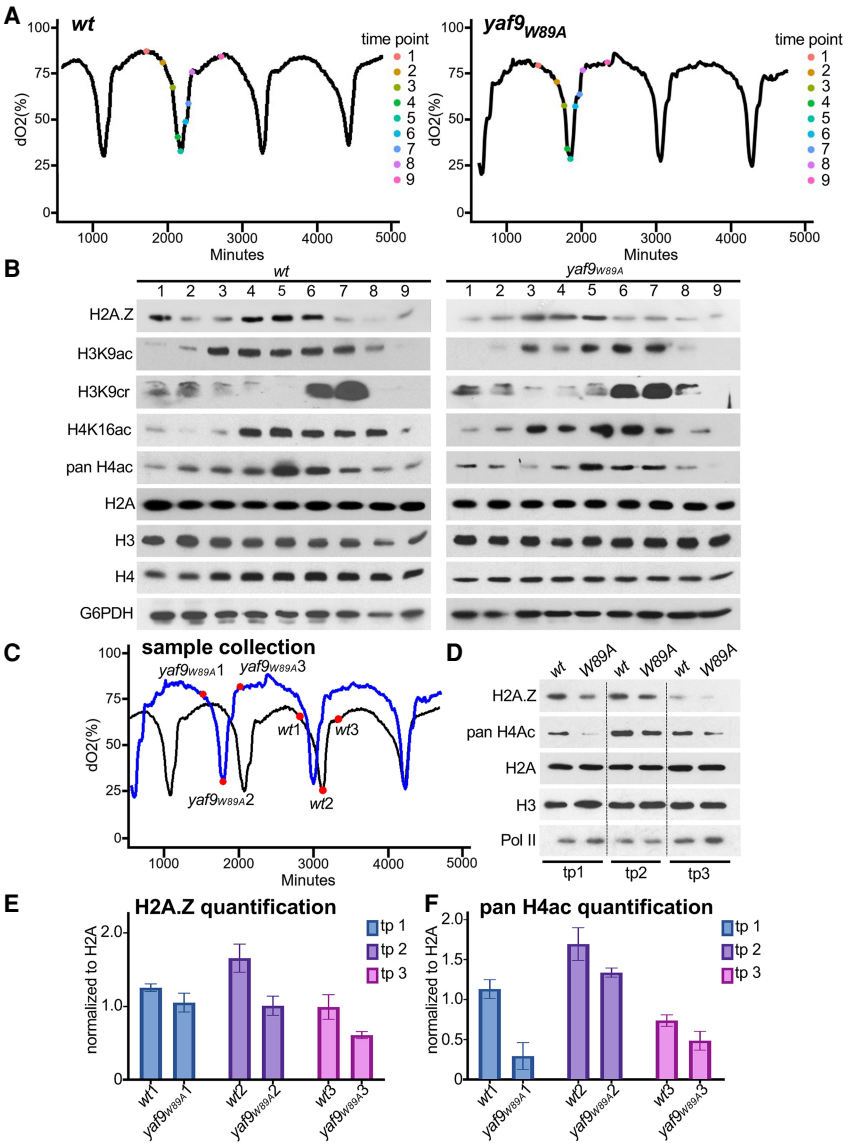

Figure 2. H2A.Z and H4 acetylation oscillate across the YMC and their levels are regulated by Yaf9-H3 acyl reading. (*A*) Nine YMC samples from wild-type and *yaf9*$_{W89A}$ strains were collected to cover one complete YMC. The collection times are indicated on the YMC profiles. A segment of a complete YMC experiment of each strain is shown to demonstrate the collection strategy and the distance between samples. (*B*) Immunoblots of wild-type and *yaf9*$_{W89A}$ YMC whole-cell lysates with the indicated antibodies. (ac) Acetylation, (cr) crotonylation. Histones H2A, H3, H4, and G6PDH are loading controls. (*C*) Overlapped wild-type (black line) and *yaf9*$_{W89A}$ (blue line) YMC profiles show the collection strategy for comparing three distinct time points between the strains. Time point 1 represents a transition point between the LOC phase and HOC phase, whereas time points 2 and 3 represent the peaks of the HOC and LOC phases. (*D*) Immunoblots of wild-type and *yaf9*$_{W89A}$ YMC whole-cell lysates to compare the time points collected in *C*. Corresponding time point samples of each strain were loaded next to each other. Histones H2A and H3 are loading controls. The blots presented are one of three independent experiments. (*E*) Bar graph showing quantification of H2A.Z levels compared with H2A control within the same time point of both strains. Error bars show standard deviation of three independent experiments ($P < 0.005$). (*F*) Bar graph showing quantification of H4ac levels compared with H2A control within the same time points for both strains. Error bars show standard deviation of three independent experiments ($P < 0.005$).

component analysis (PCA) of the results showed close correlation between the triplicates across all time points except for a possible outlier in time point 4 (Fig. 3C). The PCA plot also revealed strong similarity between the wild-type and *yaf9*$_{W89A}$ samples at time points 1, 2, and 5. However, time points 3 and 4 (transition into the LOC) showed a more distanced relationship between the wild type and *yaf9*$_{W89A}$ mutant, which suggested that greater differences in transcriptional regulation occur at time points 3 and 4.

Further examination of the RNA-seq data from the list of differentially expressed (SDE) genes revealed that time point 3 (LOC phase) had the greatest changes in gene expression between the wild-type and *yaf9*$_{W89A}$ mutant cells, with twice as many down-regulated genes (n = 1505) and up-regulated genes (n = 1467) in the *yaf9*$_{W89A}$ mutant as compared with other time points (Figu. 3D,F). Among the top SDE genes in time point 3, we observed up-regulation of genes that are involved in oxidative and progrowth pathways, including ribosome and macromolecule biosynthesis, and down-regulation of genes that are involved in reductive pathways, such as oxidation reduction process and oxidoreductase activity (Fig. 3E). These findings suggested that, in the *yaf9*$_{W89A}$ mutant, progrowth/HOC-regulated genes were not properly down-regulated during the transition into LOC phase and that the normal expression of LOC genes was attenuated during this phase.

To further understand how the *yaf9*$_{W89A}$ mutation affected HOC and LOC gene expression, we selected from the RNA-seq data a subset of genes found to be dysregulated in time point 3 and measured their expression across the YMC by quantitative reverse transcriptase (RT)-qPCR. As shown in Figure 4A, two representative HOC-phase genes, *CLN3* and *RPL18B*, showed partially reduced transcription in the *yaf9*$_{W89A}$ mutant compared with wild type at time points 1 and 2. Consistent with the RNA-seq data of these genes, the mRNA levels of *CLN3* and

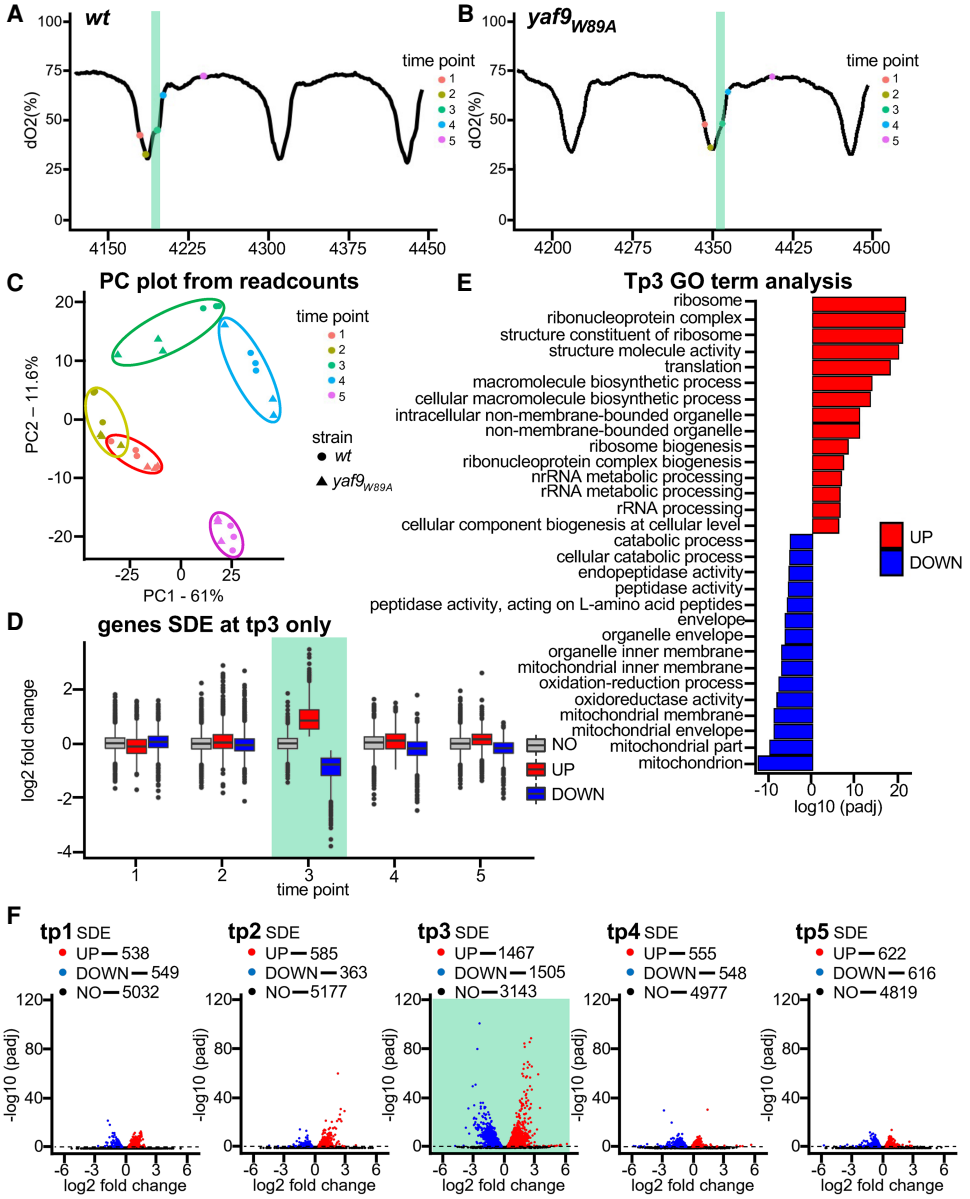

Figure 3. The YEATS domain of Yaf9 is required for precise metabolic gene transcription. (*A*,*B*) YMC traces corresponding to samples collected from wild-type and *yaf9*$_{W89A}$ strains for RNA-seq analysis. Biological triplicates of each YMC sample were collected from three consecutive cycles. Time point 3, which showed the greatest defect in gene expression from the analyses, is highlighted in green background on both YMC traces. (*C*) Principal component analysis of RNA-seq samples. Biological triplicates are shown for each time point. Each time point is indicated by one color. Wild-type samples are represented by circles, and *yaf9*$_{W89A}$ samples are represented by triangles. (*D*) Box plot of $\log_2$ fold change of SDE genes showing highest polar distribution on time point 3. Time point 3 is highlighted in green background. (*E*) DAVID functional annotation enrichment analysis of SDE genes at time point 3. Enrichment is shown as $-\log_{10}$ *P*-value. (*F*) Volcano plots showing differences in gene expression between wild type and *yaf9*$_{W89A}$. Log_2 fold expression change (*X*-axis) and $-\log_{10}$ *P*-value significance (*Y*-axis) displays up-regulated (UP) and down-regulated (DOWN) genes in *yaf9*$_{W89A}$. Up-regulated genes are represented in red, down-regulated genes are represented in blue, and unchanged genes (NO) are represented in black. Time point 3 is highlighted in green background.

RPL18B observed at time point 2 largely persisted into the LOC phase (time point 3) instead of being down-regulated as occurs in wild-type cells (Fig. 4A). In contrast to the HOC genes, a LOC gene, *MRPL10*, showed decreased transcription in the *yaf9*$_{W89A}$ mutant compared with wild-type cells at most time points across the YMC, and, notably, *MRPL10* was less expressed in the LOC phase, consistent with the RNA-seq data (Figs. 3, 4B). The findings that HOC genes maintained expression in the LOC phase and that LOC genes were not properly expressed were recapitulated for additional HOC genes (*RPS5*, *RPL4B*, and *RPL8B*), and LOC genes (*PYC1*, *SSC1*, and *TDH2*) that

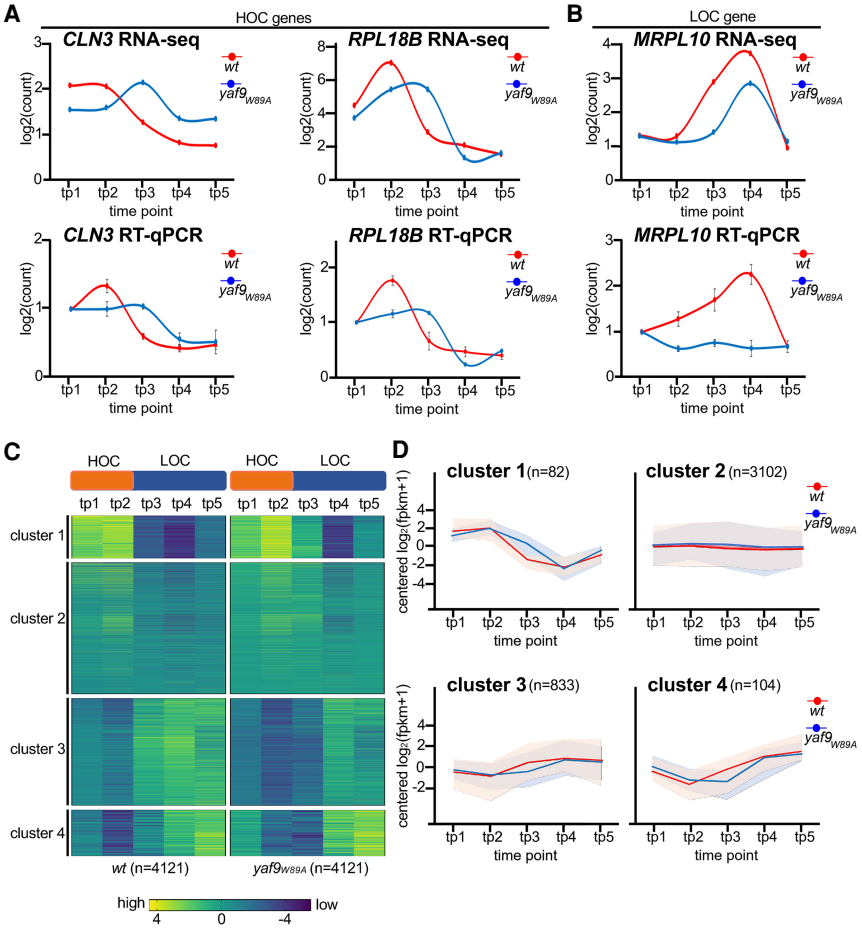

Figure 4. Individual RT-qPCR experiments coincide with the RNA-seq data. (*A*,*B*) Transcription patterns of two HOC genes and one LOC gene across the YMC are plotted using RNA-seq data for wild type and *yaf9*$_{W89A}$. RT-qPCR analysis of the same genes in wild-type and *yaf9*$_{W89A}$ YMC samples performed with targeted primers. RT-qPCR transcription patterns are plotted to compare with the RNA-seq graphs. The standard deviation of a representative experiment is shown. A total of three biological experiments was performed, each of which showed similar findings. Actin was used as the standard for signal normalization. (HOC) High oxygen consumption, (LOC) low oxygen consumption. (*C*) Unsupervised hierarchical cluster analysis of RNA-seq gene transcription ($n = 4121$) based on $\log_2$(FPKM + 1) showing four clusters. The clusters are shown in separate heat maps. Bars *above* heat maps show metabolic phase and time points collected in the phase. Color scale is shown *below* the heat maps. (*D*) Line plots showing the transcription trends of four gene clusters from hierarchical clustering. There are 4121 SDE genes, and the number of genes in each cluster is indicated. Wild-type transcription trends are represented by red solid lines, and *yaf9*$_{W89A}$ transcription trends are represented by blue solid lines. The transcription trends represented by the solid lines are the median centroids of each cluster. The transcription range of clustered genes is represented by shaded area (red for wild type, and blue for *yaf9*$_{W89A}$).

were measured by RNA-seq (Supplemental Fig. S2). Finally, several noncycling (NC) genes identified from our RNA-seq data were largely unaffected throughout the YMC in *yaf9*$_{W89A}$ mutant cells (Supplemental Fig. S2).

The results of our RNA-seq analysis so far prompted us to next determine whether the transcription defects we observed in a subset of metabolic genes in the *yaf9*$_{W89A}$ mutant occurred more broadly for other metabolically regulated and NC genes. Out of 4121 genes that showed measurable signals, we performed an unsupervised hierarchical clustering that resulted in four clusters based on their transcription profiles across the five time points (Fig. 4C,D). Cluster 1 genes ($n = 82$) were exclusively HOC-regulated (96%), whereas clusters 3 ($n = 833$) and 4 ($n = 104$) were almost exclusively LOC-regulated genes (85% and 90%, respectively). The largest group, cluster 2, contained a mixture of HOC-regulated genes ($n = 1086$, 35% of this cluster), LOC genes ($n = 910$, 29% of this cluster), and the rest ($n = 1030$) nonmetabolically regulated genes (Supplemental Table S1). Consistent with our RT-qPCR analyses, HOC-regulated genes in clusters 1 and 2 showed persistent transcription at time point 3 in the *yaf9*$_{W89A}$ cells. In contrast, all the LOC-regulated genes in clusters 3 and 4 exhibited decreased transcription during the LOC phase, which was more pronounced at time point 3 and was consistent with our box plot analyses (Figs. 3D, 4C). The line plots in Figure 4D show the average mRNA signals in wild-type or *yaf9*$_{W89A}$ mutant cells for each cluster across the YMC. These findings revealed two important observations about how the absence of Yaf9-H3 acyl reading affects metabolic gene expression. First, the normal restriction of progrowth gene expression to the HOC phase was partially lost because HOC genes maintained their expression in the LOC phase. Second, the normal induction of genes in the LOC phase was attenuated.

Yaf9-H3 acyl reading is required for proper deposition of H2A.Z and H4 acetylation at genes

To further understand how Yaf9-H3 acyl reading contributes to gene transcription, we performed chromatin immunoprecipitation (ChIP) assays coupled with quantitative PCR (ChIP-qPCR) on a subset of genes to determine whether the absence of Yaf9-H3 acyl reading affected the occupancies of H2A.Z and/or H4 acetylation. Time points from the YMC used for the ChIP-qPCR assays were the same as those used in the prior RNA-seq experiments (Fig. 3A,B). For this analysis, we selected *RPL4B* as a representative HOC gene, *SSC1* as a

representative LOC gene, and *FBA1* as a control NC gene whose transcription level was largely unaffected in the $yaf9_{W89A}$ mutant (Fig. 5A; Supplemental Fig. S3). H2A.Z and H4ac occupancy levels were examined at the −1 nucleosome, +1 nucleosome, and 3′ end of these genes (+1 nucleosome results shown in Figure 5B; the full data set is shown in Supplemental Fig. S3). In agreement with the global changes observed with H2A.Z and H4ac in bulk chromatin, the levels of H2A.Z and H4ac at all genes examined also oscillated across the YMC in wild-type cells, with levels being highest during the HOC phase (Fig. 5B). In contrast to wild-type cells, the occupancies of H2A.Z and H4ac decreased significantly in the $yaf9_{W89A}$ mutant at all time points examined (Fig. 5B; Supplemental Fig. S3). Importantly, H4ac changes were not due to changes in overall nucleosome levels, as H3 occupancy did not significantly fluctuate across the YMC or in the $yaf9_{W89A}$ mutant (Supplemental Fig. S4).

We next measured the occupancy of Pol II at the same genes described above to determine the effect of Yaf9-H3 acyl reading on Pol II occupancy levels. Strikingly, Pol II occupancy oscillated across the YMC at all genes examined in wild-type cells, with Pol II levels being lowest at the HOC phase and highest at the LOC phase (Fig. 5C; Supplemental Figs. S5, S6). To our knowledge, it has not been reported that Pol II levels are influenced by metabolic state and are anticorrelated with H2A.Z and histone acetylation levels over the YMC, although our findings are consistent with reports of antagonism between H2A.Z and Pol II during transcription (Weber et al. 2014; Tramantano et al. 2016; Ranjan et al. 2020). These findings also agree with other work showing that the nucleosome-free regions of genes are in competition between Swr1 and initiation factors for transcription (Ranjan et al. 2013; Yen et al. 2013). Pol II occupancy in the $yaf9_{W89A}$ mutant had a cycling pattern similar to Pol II in wild-types cells, albeit with reduced levels at the NC *FBA1* gene during the peak of Pol II levels in the LOC phase.

Histone binding by Yaf9 is required for SWR1-C and NuA4 chromatin recruitment

The totality of transcription and global H2A.Z/H4ac defects observed in the $yaf9_{W89A}$ strain prompted us to ask how Yaf9-H3 acyl binding contributes to the chromatin-based functions defective in $yaf9_{W89A}$. We reasoned that either Yaf9-H3 acyl binding was required for proper recruitment of the SWR1-C and NuA4 complexes to chromatin or that these complexes were already on chromatin and that Yaf9 H3-acyl binding stimulates their enzymatic activities. To test these possibilities, we performed chromatin association assays across three YMC time points that covered different locations across the HOC and LOC phases (tp1 = LOC-to-HOC transition, tp2 = HOC, and tp3 = LOC) (these being the same time points shown in Fig. 2C). Consistent with the immunoblotting analyses of whole-cell lysates (Fig. 2D), the chromatin levels of H2A.Z and H4ac were significantly reduced at all times points in the $yaf9_{W89A}$ strain compared with wild type (Fig. 6A). However, the soluble fraction (nucleoplasm and cytoplasm) did not contain any detectable H2A.Z or H4ac (Fig. 6A). As controls, we probed for H2A and H3 to monitor the chromatin fraction and G6PDH to monitor the soluble fraction. In all time points, and between strains, the levels of histones and G6PDH were unchanged (Fig. 6B). Intriguingly, the chromatin-bound form of Yaf9 was largely absent in the

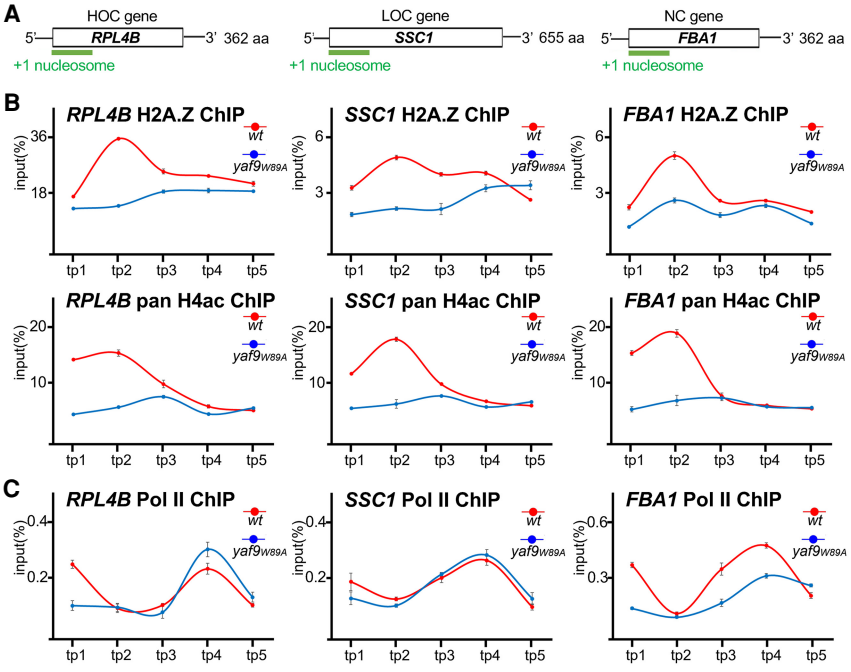

Figure 5. Yaf9-H3 acyl reading is required for proper deposition of H2A.Z and H4 acetylation at genes. (*A*) Schematic of the locations of +1 nucleosome primers on the *RPL4B*, *SSC1*, and *FBA1* genes. Each gene was selected as a representative of its metabolic gene category. (*B*) ChIP-qPCR analysis of H2A.Z and H4ac occupancies of YMC samples on selected genes showing decreased occupancies of H2A.Z and H4ac on +1 nucleosome loci of genes in $yaf9_{W89A}$ but specifically at time point 2. The YMC sample collection strategy is same as that in Figure 3, A and B. (*C*) ChIP-qPCR analysis of RNA polymerase II (Pol II) occupancy showing an opposite enrichment trend compared with H2A.Z occupancy. Standard deviation of a representative experiment is shown. Three biological experiments were performed, each of which showed similar findings. In addition to the +1 nucleosome results shown here, additional gene locations (−1 nucleosome and the 3′ end) and additional examples of others genes examined are shown in Supplemental Figures S3, S5, and S6. YMC sample collection strategy is same as that in Figure 3, A and B.

Yaf9-H3 acyl-blocking mutant and relocated to the soluble fraction (Fig. 6A). Thus, the H3 acyl binding function of Yaf9 is important for its recruitment to chromatin.

Because Yaf9's association with chromatin was dependent on its H3 acyl reading activity, we next asked whether absence of Yaf9-H3 acyl reading also influences the chromatin-association of the SWR1-C and/or NuA4 complexes that contain Yaf9. Using antibodies that specifically target members of the SWR1-C and NuA4 complexes (Swr1 and Eaf1, respectively) (Auger et al. 2008; Wu et al. 2009), we examined the levels of these complexes in our chromatin association assays as described in Figure 6A. Strikingly, although the total amounts of Swr1 and Eaf1 did not differ significantly across the three YMC time points, their chromatin levels did differ. Specifically, Eaf1 and Swr1 chromatin levels were highest in the HOC phase (tp2) and lowest in the LOC phase (tp3) (Fig. 6A). These association patterns also followed the cyclic patterns observed with histone acetylation across the YMC (Fig. 2C). In contrast to the wild-type situation, the chromatin levels of Swr1 and Eaf1 in the $yaf9_{W89A}$ samples were greatly reduced at all time points; instead, they had quantitatively relocated to the soluble fractions (Fig. 6C). Consistent with these findings, we also determined that NuA4 and SWR1-C occupancy at a number of genes tested (as monitored by the examination of Eaf1 and HA-tagged Swr1 by ChIP-qPCR) correlated well with the level of these complexes found on bulk chromatin across the YMC and in the $yaf9_{W89A}$ mutant (Supplemental Fig. S7). Finally, we note that the total amount of Eaf1 in the $yaf9_{W89A}$ samples was significantly lower compared with wild type, which explained the lower levels of Eaf1 in the chromatin and soluble fractions of $yaf9_{W89A}$. Figure 6E shows the quantified chromatin levels of Yaf9, Eaf1, and Swr1 from these experiments.

Our study of the function of Yaf9's YEATS domain also revealed a surprising observation. Although the Yaf9 YEATS domain was important to the recruitment of SWR1-C and NuA4 under nutrient-limiting conditions, the $yaf9_{W89A}$ mutant, in addition to the complete absence

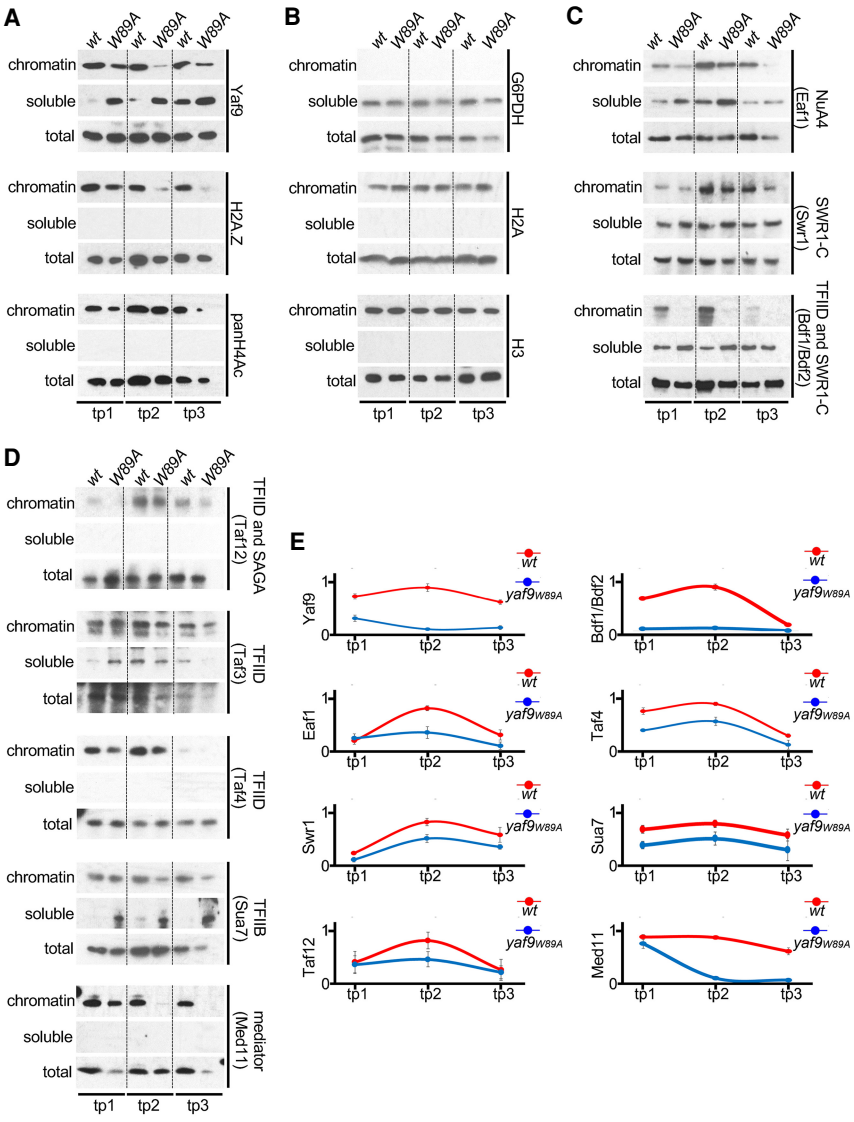

Figure 6. Histone binding by Yaf9 is required for SWR1-C and NuA4 chromatin recruitment. (*A–D*) Immunoblots of chromatin and soluble fractions from chromatin association assays. Total fractions were used as inputs. Levels of chromatin-bound Yaf9, H2A.Z, H4ac, Eaf1, Swr1, Bdf1/Bdf2, Sua7, Med11, Taf3, Taf4, Taf12, and Taf14 in wild-type and $yaf9_{W89A}$ YMC samples are shown in the chromatin fraction blots. Histones H2A, H3, and G6PDH are loading controls. The YMC sample collection strategy of the three time points is consistent with that in Figure 2C. Time point 1 from the wild-type and $yaf9_{W89A}$ YMC samples represents a transition point between the LOC phase and HOC phase, whereas time points 2 and 3 represent the peaks of the HOC and LOC phases. These time points are equivalent to those shown in Figure 2C. (*E*) Bar graphs showing quantitation of chromatin-bound Yaf9, Eaf1, Swr1, Taf12, Taf4, Med11, Sua7, and Bdf1/Bdf2 levels compared with their corresponding total fraction counterparts. Wild-type normalized chromatin-bound protein levels are indicated by red lines, and $yaf9_{W89A}$ normalized chromatin-bound protein levels are indicated by blue lines. Error bars show standard deviation of three independent experiments ($P < 0.005$).

of Yaf9, had no impact on H2A.Z or H4ac levels in the prototrophic strain grown in nutrient-rich (YPD) conditions (Supplemental Fig. S1A,B). Thus, under optimal growth conditions, Yaf9 is dispensable for the functions of SWR1-C and NuA4; its function was revealed only under more naturally occurring and nutrient-limiting growth conditions, as occurs in the wild.

The requirement of Yaf9's H3 acyl reading activity for the global recruitment of NuA4 and SWR1-C to chromatin prompted us to assess whether other aspects of the transcriptional apparatus were affected during YMC growth of the Yaf9 YEATS domain mutant. To test this possibility, we measured the levels of representative transcription initiation factors including members of the TFIID and SAGA complex (Taf3, Taf4, and Taf12), the TFIIB complex (Sua7), the mediator complex (Med11), and BET family members (Bdf1/Bdf2) that occur in the preinitiation complex (PIC) and in SWR1-C (Fig. 6C,D). Intriguingly, all the aforementioned initiation factors were localized to chromatin across all of the time points in the YMC, with their associations being highest in the HOC phase (i.e., time point 2). We also attempted to examine Pol II levels in these assays; however, the assay resulted in an unexpected loss of Pol II protein during sample processing that precluded its global examination (Supplemental Fig. S8). In contrast to the wild-type situation, the absence of Yaf9's H3 acyl interaction resulted in a global decrease in all of the initiation factors tested. The decrease was most notable for Brd1/Brd2 (see Fig. 6E for quantification of chromatin levels for several of these initiation factors).

Taken together, these findings emphasize the important function of Yaf9 and its histone reading activity in the timely recruitment and stability of transcription initiation factors and chromatin modifiers on genes during the YMC. During oxidative metabolism in which glucose levels are high, Yaf9 and its H3 reading contribute to the timely recruitment of the SWR1-C and NuA4 complexes that then establish a chromatin H2A.Z and histone acetylation signature—a signature that then reinforces further recruitment of bromodomain-containing initiation machinery for gene transcription.

Discussion

The YEATS domain has become recognized as a critical regulator of metabolic- and chromatin-based gene transcription events (Schulze et al. 2009; Li et al. 2017; Gowans et al. 2019). Intriguingly, although some YEATS domains prefer histone crotonylation (e.g., Taf14), others, such as the YEATS domain of Yaf9, bind histone acetylation and crotonylation equally (Fig. 1C). This expanded acyl selectivity may explain why, unlike Taf14, Yaf9 appears to function largely during the respiration (HOC) phase when acetyl-CoA and histone acetylation levels are highest. We also found that, during respiration, Yaf9-H3 acetyl reading mediates recruitment of its associated complexes (SWR1-C and NuA4) to install H2A.Z and H4 acetylation. The high levels of histone acetylation in the HOC phase likely act to further recruit transcriptional initiation and chromatin regulatory machinery to genes by the acetylation-driven recruitment of bromodomain-containing factors that exist in initiation and chromatin machinery. Coincident with this acetylation-dependent chromatin signature, Pol II levels were anticorrelated and decreased at genes—a finding that agreed with other reports of an antagonistic relationship between Pol II and H2A.Z, as well as other chromatin regulators, that compete with Pol II for binding to the nucleosome-free regions of genes (Yen et al. 2013; Weber et al. 2014; Tramantano et al. 2016; Ranjan et al. 2020). As yeast cycle out of the HOC phase and into the LOC phase, the pattern of chromatin and initiation factor recruitment is reversed, with Pol II levels becoming higher at genes. Thus, our study unveils an intriguing metabolic cycling of both histone PTMs and factors to genes that is dependent on the functions of Yaf9.

Different chromatin and transcription factor states for different metabolic situations

The distinct chromatin and factor recruitment states that exist at different phases of the YMC are an intriguing finding of this study. Other investigators have reported the cyclic nature of histone acetylation across the YMC on genes and globally on chromatin (Cai et al. 2011; Mellor 2016); however, our findings extend those observations to the recruitment of transcription and chromatin machinery that also associates with acetylated histones. Thus, our findings reveal that distinct chromatin- and factor-bound states are established at distinct metabolic states. A puzzling question then is why Pol II occupancy is low during the oxidative phase at a time when histone acetylation and factor recruitment is high, and why low Pol II occupancy is reversed in the reductive phase of the metabolic cycle. Perhaps one explanation for this phenomenon is that the high levels of preinitiation machinery increased on chromatin during the oxidative phase facilitates rapid reinitiation of Pol II to help achieve the high levels of transcription needed for transcription of ribosomal genes and other progrowth genes. However, this explanation might be considered at odds with findings of low Pol II levels during this phase (compared with that observed during the reductive phase) (see Fig. 5C; Supplemental Fig. S3D). The reduced occupancy of Pol II in the oxidative phase is likely a consequence of having high levels of H2A.Z, which has been shown to be anticorrelated with Pol II (Tramantano et al. 2016; Ranjan et al. 2020). We speculate that lower levels of Pol II occupancy coupled with high levels of H2A.Z may provide a controlled step of pausing during each round of transcription to ensure that the polymerase has successfully initiated and entered productive elongation. Additionally, the high H2A.Z levels may ensure proper directionality and/or prevention of inappropriate antisense transcription (Gu et al. 2015; Bagchi et al. 2020). Conversely, and during the LOC phase when histone acetylation on chromatin and initiation factors and H2A.Z levels are reduced, higher Pol II levels at this time may enable genes to overcome

the lack of abundant preinitiation machinery that is less abundant due to less histone acetylation. Thus, the cell appears to have evolved ways to overcome major differences that exist within chromatin under vastly different metabolic and cellular conditions to achieve precise and productive transcription (Fig. 7). Further work is needed to determine whether this model is correct.

Although our studies suggest that Yaf9 functions primarily during the HOC phase, we note that the absence of Yaf9-H3 acetyl reading still affects recruitment of SWR1-C and NuA4 (and other initiation and chromatin factors) in the LOC phase, albeit normally the levels recruited during this phase are much lower compared with the oxidative phase. We speculate that recruitment of SWR1-C and NuA4 during the LOC phase, albeit at low levels compared with the HOC phase, may be driven by the presence of histone crotonylation that exists during this phase (perhaps in combination with any remaining histone acetylation that also exists during this time).

Finally, the chromatin and transcription signatures described above that change across the YMC appear to occur globally for all genes transcribed in their respective YMC phases. This condition raises the question of how cells fine-tune and regulate the transcription of genes in a cyclic manner at the correct time if the chromatin and transcription signatures described here occur on all genes when they are in a particular phase. We suggest that while the chromatin and transcription initiation signatures that are found at distinct YMC phases occur broadly at genes, they do not take into account the actions of additional transcription factors that also contribute to metabolic gene transcription at each phase (both positive and negative regulation). It is likely that the transcription factors deployed at each distinct phase to activate or repress transcription do so in the context of the distinct chromatin contexts that occur in the HOC and LOC phases.

Detailing Yaf9's function: context matters

Unexpectedly, we found that the necessity of Yaf9 for NuA4 and SWR1-C recruitment to chromatin was

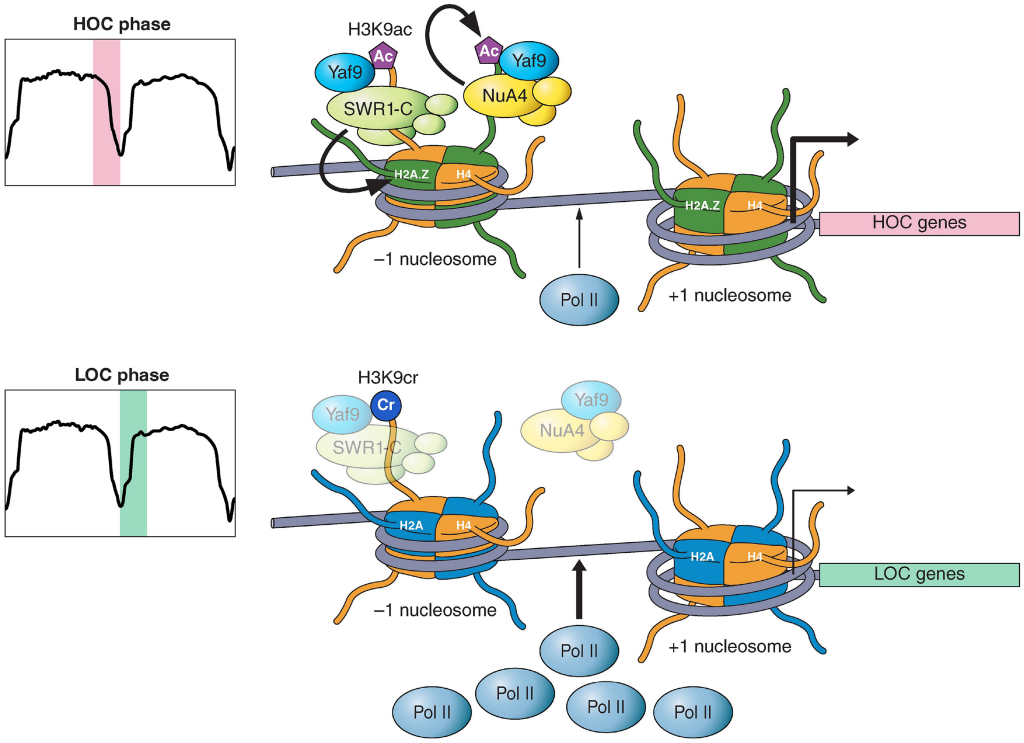

Figure 7. Model for Yaf9-H3 acyl binding regulation of the precise timing and level of metabolic gene transcription. These studies define a function for Yaf9 and its YEATS domain in chromatin and metabolic gene regulation. During respiration and oxidative metabolism, in which levels of acetyl-CoA and histone acetylation are high (the high oxygen consumption phase [HOC]), we found that Yaf9, by its reading of H3 acetylation, was required for the timely recruitment of SWR1-C and NuA4, which increase H4 acetylation and H2A.Z deposition. This phase is associated with high levels of histone acetylation-driven recruitment of bromodomain factors that include Brd1/Brd2 and other chromatin and preinitiation machinery (e.g., TFIID). However, this phase also results in reduced Pol II levels at genes. In contrast to the HOC phase, and as cells metabolically cycle into the reductive and low oxygen consumption phase (LOC), the production of acyl-CoAs is increased (e.g., histone crotonylation [cr]), and overall histone acetylation levels are dramatically reduced. The absence of histone acetylation results in reduced recruitment of Yaf9 and its associated complexes and is associated with increased occupancy of Pol II at genes compared with occupancy in the HOC phase. The function of anticorelated levels of Pol II and H2A.Z/H4ac across the YMC is not yet understood. Altogether, these findings reveal an unexpected cycling of chromatin and transcriptional initiation machinery at distinct metabolic states that likely underpins how cells precisely regulate transcription programs during nutrient flux.

bypassed when yeast was grown in nutrient-rich conditions (i.e., YPD). Consistent with this, the complete absence of Yaf9 did not have any effect on histone H4 acetylation level or H2A.Z incorporation during batch growth in YPD (Supplemental Fig. S1A). Also, Yaf9 with the H3 acyl-blocking mutation was still associated with chromatin in YPD conditions. However, in nutrient-limiting conditions, akin to what is observed in the wild, Yaf9 and its histone reading were crucial for the recruitment of NuA4 and SWR1-C (as well as other transcriptional initiation machinery) at genes. We surmise that, in a natural setting where nutrients are more limiting, Yaf9 provides a key function in facilitating SWR1-C and NuA4 recruitment that could not be achieved otherwise. In contrast, and in rich media where acetylation and other histone modifications are more abundant, it may be that the other reader domains present in NuA4 and SWR1-C complexes are simply sufficient for their recruitment. Thus, nutrient-limiting conditions may create an "all hands on deck" reader domain situation to ensure the timely and appropriate recruitment of needed chromatin and initiation machinery to chromatin when energy is limiting. If this idea is correct, it then also raises an intriguing question: How many other ancillary members of chromatin and transcription complexes have not been fully understood given most studies with yeast have been performed in optional YPD growth conditions? While our study makes this point for one member of two chromatin complexes, it will be important to consider growth conditions and cellular contexts when examining the function of chromatin and transcription machinery.

In conclusion, we revealed an important function of Yaf9 in maintenance of proper regulation of transcription across the YMC. This function is elicited by the ability of Yaf9 to read histone acetylation and facilitate the recruitment of its associated complexes that establish a chromatin and transcription initiation signature at genes required for timely transcription. Our findings also reveal that distinct mechanisms likely have evolved to regulate transcription during different nutrient and energy states, as shown by the absence of this chromatin and transcription initiation factor signature during times of low histone acetylation and low cellular energy. Because metabolic pathways are often highjacked in cancer, it will be intriguing to determine whether the activities we observed are conserved and dysregulated in cancer.

Materials and methods

Yeast strains and metabolic cycling

Saccharomyces cerevisiae strains generated for this study were created in the CEN.PK background. These and other strains used are listed in Supplemental Table S2. CEN.PK was verified to have mitochondria as indicated by the ability to grow on glycerol-containing media. The $yaf9_{W89A}$ strain was constructed using the delitto perfetto system (Klein et al. 2018a). Yeast metabolic cycling conditions were applied as described with minor adjustments (Gowans et al. 2019). Dissolved oxygen percent in media shown in YMC plots is relative to starting culture conditions (~100%). Continuous respiration cycles occur following addition of 0.15% glucose to starved cells. For each experiment, the time (in minutes) is shown relative to the start of the experiment. Spotting assays were performed by plating serial dilutions (1:5) of the indicated strains on YP media containing either 2% glucose (YPD), 3% glycerol (YPG), 80 µg/mL 6-azauracil on synthetic complete minus uracil plates (SC−Ura), 100 mM caffeine, 50 mM methanemethyl sulfonate, or 25 mM phleomycin and grown at 30°C or 37°C.

Immunoblotting

Cultures were collected from the YMC and immediately snap-frozen in liquid nitrogen. Samples for immunoblotting were fixed in 20% trichloroacetic acid after thawing and washing once in water. The protocol of Kushnirov (2000) was used to extract protein from samples. Standard conditions were used for SDS-PAGE and immunoblotting. Antibodies used in this study were as follows: anti-H2A.Z (1:10,000; Active Motif 39647), anti-H3K9 acetylation (1:2000; Millipore 06-942), anti-H3K9 crotonylation (1:500; PTM Biolabs PTM 527), anti-H4K16 acetylation (1:2000; Millipore 07-329), anti-pan H4 acetylation (1:1000; Active Motif 39925), anti-H2A (1:10,000; Active Motif 39235), anti-H3 (1:5000; Epicypher 13-0001), anti-H4 (1:1000; RevMAb 31-1089-00), anti-G6PDH (1:10,000; Sigma A9521-1VL), anti-polymerase II (1:1000; Millipore 05-623), anti-Yaf9 (1:5000; Pocono rabbit farm), anti-Eaf1 (1:1000; Côté laboratory), anti-Swr1 (1:500; Wu laboratory), anti-Sua7 (1:1000; Gene Tex GTX64172), anti-Med11(1:500; Gene Tex GTX64137), anti-Pol II (1:10,000; Gross laboratory), anti-Bdf1/Bdf2 (1:1000; Govin laboratory), anti-Taf4 (1:1000; Weil laboratory), anti-Taf12 (1:1000; Hahn laboratory), anti-HA (1:1000; Proteintech 51064-2-AP), and anti-Taf14 (1:5000; Reese laboratory).

RNA-seq analysis

RNA was prepared from samples (~10 ODs) using the RNA extraction method. The sequencing libraries were from Gowans et al. (2019), and the sequencing was performed by Novogene. Triplicates of samples were combined for final analysis. Principal component analysis plots (log transformed data) and significantly differentially expressed (SDE) genes (adjusted P-value < 0.05 and $\log_2$ fold change > 0.6) were generated using the DESeq2 package (Gowans et al. 2019). Gene ontology (GO) term analysis was performed for SDE genes with default parameters to identify enriched genes. The numbers of genes with large and statistically significant fold changes are presented in volcano plots. Line graphs were generated from the four hierarchical cluster lists provided by the analysis from the Novogene company. Heat maps of the four clusters were generated by Prism.

RNA extraction and reverse transcriptase (RT)-qPCR

Yeast samples were collected and snap-frozen as described with minor modifications (Gowans et al. 2019). Pellets were washed in water and resuspended in 400 µL of TES buffer (10 mM Tris HCl at pH 7.5, 10 mM EDTA, 0.5% SDS). An equal volume of acid phenol was added, and samples were vortexed for 30 sec. Samples were then incubated for 45 min at 65°C with occasional vortexing before being chilled for 1 min on ice. Samples were centrifuged at 12,000 RPM for 5 min at 4°C, and the upper phase was transferred to a fresh tube. Phenol extractions were repeated twice. RNA was precipitated by adding 0.1 vol of 5 M sodium acetate (pH 5.3) and 2.5 vol of 100% ice-cold ethanol followed by

incubation for 1 h at −80°C. Samples were centrifuged at 12,000 RPM for 5 min at 4°C, and pellets were washed with 70% ice-cold ethanol. Pellets were resuspended in water, and the concentrations were measured. RNA (10 mg) was treated with RQ1 DNase (Promega Corporation M6101) for 60 min at 37°C. RNA was purified using RNeasy mini kit (Qiagen 74104). cDNA was prepared using iScript cDNA synthesis kit (Thermo Fisher Scientific 18080051). qPCR was performed using the SYBR Green kit (PowerUp SYBR Green master mix, Bio-Rad 170 8880), and the primers are listed in Supplemental Table S3. Actin was used as the standard for signal normalization.

Chromatin immunoprecipitation (ChIP)

Antibodies used for ChIP were as follows: anti-H3 (Epicypher 13-0001), anti-H2A.Z (Active Motif 39647), anti-Eaf1 (Côté laboratory), anti-HA (Proteintech 51064-2-AP), anti-H3K9 acetylation (Millipore 06-942), anti-polymerase II (Millipore 05-623), and anti-Yaf9 (Pocono rabbit farm). Chemostat samples (40 mL of saturated culture) were collected, fixed in 1% formaldehyde for 15 min, and quenched in 125 mM glycine for 10 min. Cells were washed twice in TBS (300 mM NaCl, 40 mM Tris at pH 7.5) and snap-frozen. Pellets were resuspended in 500 uL of FA buffer (50 mM HEPES at pH 7.5, 140 mM NaCl, 1% Triton X-100, 1 mM EDTA, 0.1% sodium deoxycholate, Roche Complete protease inhibitor cocktail) and lysed by bead beating for 15 min at 4°C. Aliquot volumes were adjusted to 1 mL with FA buffer and sonicated (30 sec on, 30 sec off) for 25 min. Samples were pelleted at 13,000 RPM for 20 min at 4°C, and the supernatants (whole-cell lysate) were pooled. Lysates (adjusted to 2 mg/mL protein for both histones marks, H3, H2A.Z, Yaf9, HA, Eaf1, and Pol II, using FA buffer) were precleared using Dynabeads Protein A (10001D; 50 µL of beads per 500 µL of lysate, for 1 h at 4°C), and 50 µL was saved as input. Antibody was added and samples were rotated overnight at 4°C. Dynabeads were washed three times in FA buffer + 0.5% BSA, with the third wash rotated overnight at 4°C to preblock beads (50 µL per 500-µL sample). Beads were then resuspended in 200 µL of FA buffer and added to lysate samples incubated for 2 h at 4°C. Beads added to lysates were washed as follows: FA buffer, FA buffer containing 500 mM NaCl, LiCl (10 mM Tris-HCl at pH 8.0, 250 mM LiCl, 0.5% NP-40, 0.5% sodium deoxycholate, 1 mM EDTA), and 1 mL of TE (pH 8.0). Beads were resuspended in 100 µL of elution buffer (1% SDS, 0.1 M $NaHCO_3$), and DNA was eluted by shaking for 15 min at 65°C. Supernatant was collected and the elution step was repeated to yield 200 µL of eluate. Cross-links were reversed by adding 10 µL of 5 M NaCl to the eluate and incubating overnight at 65°C with shaking. Elution buffer (150 µL) was added to 50 µL of input samples and 10 µL of NaCl alongside the IP samples. Samples were treated with 10 µg of RNase A for 60 min at 37°C and then 20 µg of proteinase K for 60 min at 42°C. DNA was purified using the ChIP DNA Clean & Concentrator (Genesee/Zymo Research 11-379C/D5205) and eluted in 60 µL of elution buffer.

Chromatin association assay

Chemostat samples were collected and pelleted. Pellets were washed in water and chilled SB buffer (1 M sorbitol, 20 mM Tris HCl at pH 7.4). Pellets were collected at 3000 RPM for 5 min at 4°C and resuspended in 1.5 mL of PSB buffer (20 mM Tris HCL at pH 7.4, 2 mM EDTA, 100 mM NaCl, 10 mM β-ME) with rotation for 10 min at ambient temperature. Pellets were collected at 9000 RPM for 5 min at room temperature and washed in 1.5 mL of SB buffer at 9000 RPM for 5 min at room temperature, and then resuspended in 1 mL of SB buffer with zymolyase (10 mg/mL in SB). Samples were incubated for 1 h at room temperature. SB buffer (600 uL) was added to stop the reaction. Spheroplasts were collected at 2000 RPM for 5 min at 4°C and washed twice in 1 mL of LB buffer (0.4 M sorbitol, 150 mM potassium acetate, 2 mM magnesium acetate, 20 mM PIPES at pH 6.8) with 1 mM PMSF and a protease inhibitor cocktail tablet (Roche 11836170001). Spheroplasts were resuspended in 250 µL of LB buffer with 1 mM PMSF, one protease inhibitor cocktail, and 1% Triton-X, and incubated with occasional mixing for 10 min on ice. Samples (125 µL) were transferred to tubes labeled "total fraction"; the other 125 µL of sample was transferred to tubes labeled "chromatin fraction." Lysates in the chromatin fraction tubes were centrifuged at 5000 RPM for 15 min at 4°C, and supernatants were transferred to tubes labeled "soluble fraction." Pellets in the chromatin fraction tubes were washed three times in 1 mL of LB buffer with 1 mM PMSF, one protease inhibitor cocktail, and 1% Triton-X. Pellets were collected after washes at 5000 RPM for 5 min at 4°C, and supernatants were aspirated. Chromatin fraction sample pellets were resuspended in 125 µL of LB buffer.

Accession numbers

The accession numbers for the RNA-seq data set reported here are through GEO (accession no. GSE189089).

Competing interest statement

B.D.S. is a cofounder and scientific advisory board member of EpiCypher, Inc.

Acknowledgments

We thank members of the Strahl labroatory for suggestions and helpful discussions. We also thank Jerome Govin for the Bdf1/2 antibody, Steve Hahn for Taf antibodies, David Gross for rabbit Pol II antibody, Carl Wu for Swr1 antibody, and Jacques Côté for Eaf1 antibody. We also thank Jake Bridgers for help in Yaf9 strain construction. This work was supported by a National Institutes of Health grant to BDS (GM126900)

Author contributions: J.Z. and B.D.S. conceived the project. A.G. performed immunoblotting for Figure 2D. J.Z. collected YMC time points and performed the spotting assays, peptide pull-down assays, immunoblotting analysis, ChIP-qPCR, RT-qPCR, and chromatin association assays. J.Z. analyzed the RNA-seq data. J.Z. and B.D.S. wrote the manuscript with editorial suggestions from Howard Fried.

References

Allfrey VG, Faulkner R, Mirsky AE. 1964. Acetylation and methylation of histones and their possible role in the regulation of RNA synthesis. *Proc Natl Acad Sci* **51:** 786–794. doi:10.1073/pnas.51.5.786

Altaf M, Auger A, Monnet-Saksouk J, Brodeur J, Piquet S, Cramet M, Bouchard N, Lacoste N, Utley RT, Gaudreau L, et al. 2010. NuA4-dependent acetylation of nucleosomal histones H4 and H2A directly stimulates incorporation of H2A.Z by the SWR1 complex. *J Biol Chem* **285:** 15966–15977. doi:10.1074/jbc.M110.117069

Andrews FH, Shinsky SA, Shanle EK, Bridgers JB, Gest A, Tsun IK, Krajewski K, Shi X, Strahl BD, Kutateladze TG. 2016a.

The Taf14 YEATS domain is a reader of histone crotonylation. *Nat Chem Biol* **12:** 396–398. doi:10.1038/nchembio.2065

Andrews FH, Strahl BD, Kutateladze TG. 2016b. Insights into newly discovered marks and readers of epigenetic information. *Nat Chem Biol* **12:** 662–668. doi:10.1038/nchembio.2149

Auger A, Galarneau L, Altaf M, Nourani A, Doyon Y, Utley RT, Cronier D, Allard S, Côté J. 2008. Eaf1 is the platform for NuA4 molecular assembly that evolutionarily links chromatin acetylation to ATP-dependent exchange of histone H2A variants. *Mol Cell Biol* **28:** 2257–2270. doi:10.1128/MCB.01755-07

Bagchi DN, Battenhouse AM, Park D, Iyer VR. 2020. The histone variant H2A.Z in yeast is almost exclusively incorporated into the +1 nucleosome in the direction of transcription. *Nucleic Acids Res* **48:** 157–170.

Barnes CE, English DM, Cowley SM. 2019. Acetylation & Co: an expanding repertoire of histone acylations regulates chromatin and transcription. *Essays Biochem* **63:** 97–107. doi:10.1042/EBC20180061

Cai L, Sutter BM, Li B, Tu BP. 2011. Acetyl-CoA induces cell growth and proliferation by promoting the acetylation of histones at growth genes. *Mol Cell* **42:** 426–437. doi:10.1016/j.molcel.2011.05.004

Gardner KE, Allis CD, Strahl BD. 2011. Operating on chromatin, a colorful language where context matters. *J Mol Biol* **409:** 36–46. doi:10.1016/j.jmb.2011.01.040

Gerhold CB, Hauer MH, Gasser SM. 2015. INO80-C and SWR-C: guardians of the genome. *J Mol Biol* **427:** 637–651. doi:10.1016/j.jmb.2014.10.015

Gowans GJ, Bridgers JB, Zhang J, Dronamraju R, Burnetti A, King DA, Thiengmany AV, Shinsky SA, Bhanu NV, Garcia BA, et al. 2019. Recognition of histone crotonylation by Taf14 links metabolic state to gene expression. *Mol Cell* **76:** 909–921.e3. doi:10.1016/j.molcel.2019.09.029

Gu M, Naiyachit Y, Wood TJ, Millar CB. 2015. H2a.Z marks antisense promoters and has positive effects on antisense transcript levels in budding yeast. *BMC Genomics* **16:** 99. doi:10.1186/s12864-015-1247-4

Henikoff S, Smith MM. 2015. Histone variants and epigenetics. *Cold Spring Harb Perspect Biol* **7:** a019364. doi:10.1101/cshperspect.a019364

Hiltunen JK, Mursula AM, Rottensteiner H, Wierenga RK, Kastaniotis AJ, Gurvitz A. 2003. The biochemistry of peroxisomal β-oxidation in the yeast *Saccharomyces cerevisiae*. *FEMS Microbiol Rev* **27:** 35–64. doi:10.1016/S0168-6445(03)00017-2

Hsu CC, Shi J, Yuan C, Zhao D, Jiang S, Lyu J, Wang X, Li H, Wen H, Li W, et al. 2018a. Recognition of histone acetylation by the GAS41 YEATS domain promotes H2A.Z deposition in non-small cell lung cancer. *Genes Dev* **32:** 58–69. doi:10.1101/gad.303784.117

Hsu CC, Zhao D, Shi J, Peng D, Guan H, Li Y, Huang Y, Wen H, Li W, Li H, et al. 2018b. Gas41 links histone acetylation to H2A.Z deposition and maintenance of embryonic stem cell identity. *Cell Discov* **4:** 28. doi:10.1038/s41421-018-0027-0

Klein BJ, Vann KR, Andrews FH, Wang WW, Zhang J, Zhang Y, Beloglazkina AA, Mi W, Li Y, Li H, et al. 2018a. Structural insights into the π-π-π stacking mechanism and DNA-binding activity of the YEATS domain. *Nat Commun* **9:** 4574. doi:10.1038/s41467-018-07072-6

Klein BJ, Ahmad S, Vann KR, Andrews FH, Mayo ZA, Bourriquen G, Bridgers JB, Zhang J, Strahl BD, Côté J, et al. 2018b. Yaf9 subunit of the NuA4 and SWR1 complexes targets histone H3K27ac through its YEATS domain. *Nucleic Acids Res* **46:** 421–430. doi:10.1093/nar/gkx1151

Klevecz RR, Bolen J, Forrest G, Murray DB. 2004. A genomewide oscillation in transcription gates DNA replication and cell cycle. *Proc Natl Acad Sci* **101:** 1200–1205. doi:10.1073/pnas.0306490101

Kobor MS, Venkatasubrahmanyam S, Meneghini MD, Gin JW, Jennings JL, Link AJ, Madhani HD, Rine J. 2004. A protein complex containing the conserved Swi2/Snf2-related ATPase Swr1p deposits histone variant H2A.Z into euchromatin. *PLoS Biol* **2:** E131. doi:10.1371/journal.pbio.0020131

Bönisch C, Hake SB. 2012. Histone H2A variants in nucleosomes and chromatin: more or less stable? *Nucleic Acids Res* **40:** 10719–10741. doi:10.1093/nar/gks865

Kushnirov VV. 2000. Rapid and reliable protein extraction from yeast. *Yeast* **16:** 857–860. doi:10.1002/1097-0061(20000630)16:9<857::AID-YEA561>3.0.CO;2-B

Li Y, Zhao D, Chen Z, Li H. 2017. YEATS domain: linking histone crotonylation to gene regulation. *Transcription* **8:** 9–14. doi:10.1080/21541264.2016.1239602

Mellor J. 2016. The molecular basis of metabolic cycles and their relationship to circadian rhythms. *Nat Struct Mol Biol* **23:** 1035–1044. doi:10.1038/nsmb.3311

Mizuguchi G, Shen X, Landry J, Wu WH, Sen S, Wu C. 2004. ATP-driven exchange of histone H2AZ variant catalyzed by SWR1 chromatin remodeling complex. *Science* **303:** 343–348. doi:10.1126/science.1090701

Ranjan A, Mizuguchi G, FitzGerald PC, Wei D, Wang F, Huang Y, Luk E, Woodcock CL, Wu C. 2013. Nucleosome-free region dominates histone acetylation in targeting SWR1 to promoters for H2A.Z replacement. *Cell* **154:** 1232–1245. doi:10.1016/j.cell.2013.08.005

Ranjan A, Nguyen VQ, Liu S, Wisniewski J, Kim JM, Tang X, Mizuguchi G, Elalaoui E, Nickels TJ, Jou V, et al. 2020. Live-cell single particle imaging reveals the role of RNA polymerase II in histone H2A.Z eviction. *Elife* **9:** e55667. doi:10.7554/eLife.55667

Rothbart SB, Strahl BD. 2014. Interpreting the language of histone and DNA modifications. *Biochim Biophys Acta* **1839:** 627–643. doi:10.1016/j.bbagrm.2014.03.001

Sabari BR, Tang Z, Huang H, Yong-Gonzalez V, Molina H, Kong HE, Dai L, Shimada M, Cross JR, Zhao Y, et al. 2015. Intracellular crotonyl-CoA stimulates transcription through p300-catalyzed histone crotonylation. *Mol Cell* **58:** 203–215. doi:10.1016/j.molcel.2015.02.029

Schulze JM, Wang AY, Kobor MS. 2009. YEATS domain proteins: a diverse family with many links to chromatin modification and transcription. *Biochem Cell Biol* **87:** 65–75. doi:10.1139/O08-111

Schulze JM, Wang AY, Kobor MS. 2010. Reading chromatin: insights from yeast into YEATS domain structure and function. *Epigenetics* **5:** 573–577. doi:10.4161/epi.5.7.12856

Strahl BD, Allis CD. 2000. The language of covalent histone modifications. *Nature* **403:** 41–45. doi:10.1038/47412

Talbert PB, Henikoff S. 2021. Histone variants at a glance. *J Cell Sci* **134:** jcs244749. doi:10.1242/jcs.244749

Tramantano M, Sun L, Au C, Labuz D, Liu Z, Chou M, Shen C, Luk E. 2016. Constitutive turnover of histone H2A.Z at yeast promoters requires the preinitiation complex. *Elife* **5:** e14243. doi:10.7554/eLife.14243

Tu BP, McKnight SL. 2006. Metabolic cycles as an underlying basis of biological oscillations. *Nat Rev Mol Cell Biol* **7:** 696–701. doi:10.1038/nrm1980

Tu BP, McKnight SL. 2007. The yeast metabolic cycle: insights into the life of a eukaryotic cell. *Cold Spring Harb Symp Quant Biol* **72:** 339–343. doi:10.1101/sqb.2007.72.019

Tu BP, Kudlicki A, Rowicka M, McKnight SL. 2005. Logic of the yeast metabolic cycle: temporal compartmentalization of cellular processes. *Science* **310:** 1152–1158. doi:10.1126/science.1120499

Tu BP, Mohler RE, Liu JC, Dombek KM, Young ET, Synovec RE, McKnight SL. 2007. Cyclic changes in metabolic state during the life of a yeast cell. *Proc Natl Acad Sci* **104:** 16886–16891. doi:10.1073/pnas.0708365104

Verdin E, Ott M. 2015. 50 years of protein acetylation: from gene regulation to epigenetics, metabolism and beyond. *Nat Rev Mol Cell Biol* **16:** 258–264. doi:10.1038/nrm3931

Wang AY, Schulze JM, Skordalakes E, Gin JW, Berger JM, Rine J, Kobor MS. 2009. Asf1-like structure of the conserved Yaf9 YEATS domain and role in H2A.Z deposition and acetylation. *Proc Natl Acad Sci* **106:** 21573–21578. doi:10.1073/pnas.0906539106

Weber CM, Ramachandran S, Henikoff S. 2014. Nucleosomes are context-specific, H2A.Z-modulated barriers to RNA polymerase. *Mol Cell* **53:** 819–830. doi:10.1016/j.molcel.2014.02.014

Wu WH, Wu CH, Ladurner A, Mizuguchi G, Wei D, Xiao H, Luk E, Ranjan A, Wu C. 2009. N terminus of Swr1 binds to histone H2AZ and provides a platform for subunit assembly in the chromatin remodeling complex. *J Biol Chem* **284:** 6200–6207. doi:10.1074/jbc.M808830200

Yen K, Vinayachandran V, Pugh BF. 2013. SWR-C and INO80 chromatin remodelers recognize nucleosome-free regions near +1 nucleosomes. *Cell* **154:** 1246–1256. doi:10.1016/j.cell.2013.08.043

Zhang H, Richardson DO, Roberts DN, Utley R, Erdjument-Bromage H, Tempst P, Côté J, Cairns BR. 2004. The Yaf9 component of the SWR1 and NuA4 complexes is required for proper gene expression, histone H4 acetylation, and Htz1 replacement near telomeres. *Mol Cell Biol* **24:** 9424–9436. doi:10.1128/MCB.24.21.9424-9436.2004

Zhang Q, Zeng L, Zhao C, Ju Y, Konuma T, Zhou MM. 2016. Structural insights into histone crotonyl-lysine recognition by the AF9 YEATS domain. *Structure* **24:** 1606–1612. doi:10.1016/j.str.2016.05.023

Zhao D, Guan H, Zhao S, Mi W, Wen H, Li Y, Zhao Y, Allis CD, Shi X, Li H. 2016. YEATS2 is a selective histone crotonylation reader. *Cell Res* **26:** 629–632. doi:10.1038/cr.2016.49

Zhao D, Li Y, Xiong X, Chen Z, Li H. 2017. YEATS domain—a histone acylation reader in health and disease. *J Mol Biol* **429:** 1994–2002. doi:10.1016/j.jmb.2017.03.010